ISSN: 0067-2904

Plasma Optical Emission Spectroscopy Study of Some Iron Meteorites

Hussein Omran Hussein*, Waleed Ibrahim Yaseen
Department of Astronomy and Space -College of Science- University of Baghdad, Baghdad, Iraq

Received: 4/2/2023 Accepted: 19/5/2023 Published: 30/5/2024

Abstract

This study aims to analyze spectra in real-time for λ Draconids, σ Hydrids, μ Virginid, and one sporadic meteor using spectroscopic chemical analysis and diagnose plasma parameters. Good-resolution spectroscopy and a CCD camera for meteor observation were used concurrently to examine the ablation spectra of these meteorites in situ. The Boltzmann and Lorentz methods were then used to determine the temperature and density of electrons, the length of Debye, and the frequency of plasma. Furthermore, spectra data can be analyzed and compared to data from other sources. Spectrum tests can be utilized to identify the chemical structure of meteorites' plasma.

Keywords: Techniques: spectroscopic – meteorites, meteors, plasmas meteoroids, plasma parameters.

دراسة مطيافية الانبعاث الضوئي للبلازما لبعض النيازك الحديدية

حسين عمران حسين ، وليد ابراهيم ياسين*
قسم الفلك والفضاء، كلية العلوم، جامعة بغداد، بغداد، العراق

الخلاصة

تهدف هذه الدراسة إلى تحليل الأطياف في الوقت الحقيقي لـ λ Draconids و σ Hydrids و μ Virginid ونيزك واحد متقطع باستخدام التحليل الكيميائي الطيفي وتشخيص معلمات البلازما. تم استخدام التحليل الطيفي عالي الدقة وكاميرا CCD لمراقبة النيزك بشكل متزامن لفحص أطياف الاجتثاث لهذه النيازك في الموقع. ثم تم استخدام طريقتي بولتزمان ولورينتز لتحديد درجة حرارة الإلكترونات وكثافة الإلكترونات وطول ديباي وتكرار البلازما. بالإضافة إلى ذلك ، يمكن تحليل ومقارنة بيانات الأطياف بمصادر أخرى. يمكن استخدام اختبارات الطيف لتحديد التركيب الكيميائي لبلازما النيازك

1. Introduction

As they provide tangible planetary samples, meteorite falls with well-recorded atmospheric trajectories are crucial for planetary science. The before-impact orbit of the meteoroid in the solar system may be determined and a potential relationship to its parent body might well be established with the proper registration of a fireball entrance. [1]**.** According to some estimates, 10^8 kg of interplanetary dust of space and particles every year, primarily of Chondritic origin, are referred to as meteoroids [2]. The size (diameter) and mass distribution

*Email: waleedib1972cnc@gmail.com

of around $2x10^{-4}$ m and 10 μg influence the Earth's atmosphere [3]. A meteor is a bright event that occurs when an object reaches the Earth's atmosphere [4].

A meteoroid loses its original mass by sputtering as it enters the upper atmosphere of the planet [5]. Sputtering is the process of metallic targets ejecting material while being surrounded by chemically reactive gases whose mass interacts with both the target surface and the material being ejected [6]. Due to high-energy collisions with molecules of rarefied atmospheric gas, the meteoroid experiences fast heating and consequent differential ablation when it contacts the exponentially rising air density at lower altitudes [7]. In the Earth's atmosphere, meteoroids mostly come from two sources [8]. The first is the cometary dust trails, which are the source of meteor showers like the Perseids and Leonids, as they orbit the sun. The second are pieces from the asteroid belt behind Mars and dust from extensive cometary tails that have long since disintegrated. These cause random meteoroids to enter the system continuously. Only a massive body can create some tiny pieces on the Earth's surface at greater velocities, where the meteoroid's capacity to enter the atmosphere is highly correlated with its velocity. The word "ablation" refers to the mass loss of a meteoroid in any shape or phase, including solid pieces, liquid droplets, and loss of hot gas, which always constitutes the last stage and is what causes the meteor phenomenon that is viewed [9]. Nevertheless, ablation only occurs when a particle can reach high enough temperatures [10]. Because micrometeoroids are vulnerable to fast heat loss by heat transfer [11]. Only meteoroids with weights more than 10^{-7} g and diameters bigger than 10^{-6} m reach fusion temperatures [10]. The basic, specific elemental studies and properties of meteoroids and their origin bodies may be performed using the in-depth study of meteor spectra. Early research has concentrated on the recognition and comparison of intensity levels of the dominant spectral lines, like Fe, Cr, Ca, Mg, and Na, or other elements such as H, Li, Al, Si, Ca, Ti, Cr, Mn, Co, Ni, or Sr, rather than detailed descriptions of actual quantitative chemical compositions [12]. Typically, elemental abundances in meteors plasma are quantitatively analyzed by comparing calculated and observed spectra [13]. This process is extremely difficult and calls for extensive databases of spectral properties for every element, like NIST, as well as a deep knowledge of the optical behavior of the meteor plasma [14]. In the 19th century, meteor spectra were first studied [15]. Notwithstanding this, systematic photography and video graphic research began in the centuries that followed, with significant spectroscopic studies that were and are still being conducted in Europe and North America [16].

2. Optical Emission Spectroscopy Technique

The OES approach is widely used to diagnose plasmas in the laboratory and in nature to evaluate plasma properties such as the density of electrons, the temperature of electrons, material identification, and quantification of components in the plasma [17]. Because it requires no light source, optical emission spectroscopy is more readily suited for real-time control and monitoring than other optical diagnostics. It is feasible to have very high spatial and temporal resolutions [18]. The following is a summary of the data processing: (LTE) Local-Thermodynamic-Equilibrium is attained in both temporal and locative monitoring windows in plasma under certain conditions, and the plasma is taken to be indicative of the structure of the unperturbed target composition. In this scenario, it is reasonable to suppose that plasma is a spatially uniform source of radiation. The calculation includes optically thin spectral lines that, if measured, can be detected and separated, and represent all elements found in the target. Excited levels are staffed in accordance with the distribution of Boltzmann and the states of ionization verify the Saha-Boltzmann equilibrium equation [19].
If the level populations are distributed in accordance with the Boltzmann equation, then the relative intensity of the emission line in the LTE plasma is given by [17]:

$$ln\left(\frac{\lambda I}{A_{ki}g_k}\right) = C - \frac{E_k}{kT_e} \quad (1)$$

where I, λ, A_{ki}, g_k, E_k, k and T_e are relative intensity, wavelength, coefficient of transition probability, statistical weight for level k, upper-level energy, Boltzmann constant, and electron temperature, respectively. C is a constant in the present experimentation that is very small, therefore it is neglected. Fast-moving electrons and relatively slow-moving ions create electrical fields that have an impact on the emission type (ions or atoms) in plasma. This disruptive electrical field affects atoms or ions, creating a change in their energy levels, and that result in the Stark widening of plasma emission lines. The electron density may be determined using the Stark-broadening emission line's spectral line width. In our case, the spectral line width is dominated by the Stark-widening effect rather than Doppler collision broadening, or instrumental broadening. The Stark-broadened line full-width at half maximum (FWHM) is a measure of the electron density and is provided by [20]:

$$\Delta\lambda_{\frac{1}{2}} = 2\omega\left(\frac{n_e}{10^{16}}\right) \quad (2)$$

Where n_e is density of electron (cm^{-3}), and ω is the electron impact width parameter, which is taken from [21].

3. Debye length

In plasma, electrons are drawn to nearby ions, protecting their electrostatic fields from the surrounding plasma. Similar to this, an electron at rest draws ions and repels other electrons. The potential of a charged particle's immediate surroundings is changed by this phenomenon. A surplus of either positive or negative particles in plasma would produce an electric field, and the electrons would then migrate to neutralize the charge [22]. Debye shielding, which gives the plasma its quasi-neutral property, is the way charged particles react to lessen the impact of local electric fields. The Debye length, also known as the electric potential developed, is a measurement of how far from the particle's surface the electric potential is located. It is determined by:

$$\lambda_D = \left(\frac{\varepsilon_o k T_e}{n_e e^2}\right)^{\frac{1}{2}} \quad (3)$$

The first prerequisite for plasma existence is that the Debye length should be extremely tiny in relation to the system dimension: $\lambda_D << L$, where L is the dimension system (cm), e is the electron charge, ε_o is the free-space permittivity, and k is the Boltzmann constant [23].
m_e is the electron mass. The plasma frequency can be calculated as [24]:

$$\omega_p = \sqrt{\frac{n_e e^2}{\varepsilon_o m_e}} \quad (4)$$

4. Calculations

4.1. Determining the Meteor Spectrum

The meteor spectra obtained using (EDMOND) European video Meteor Observation Network database are shown in Figure 1. It primarily shows the brightest meteor spectra. For the purpose of calculating the trajectory and orbit, the meteors were captured concurrently by additional AMOS stations. Four meteorites can be identified (Draconids, σ Hybrids, μ Virginia, and one Sporadic meteor number of these meteorites: No.1, No.3, No.8, and No.32, respectively).

4.2. Electron Temperature Calculations

Can be assumed $T_e=T_{ion}=T_{plasma,}$ therefore all temperatures are considered to be equal, and can be calculated by Eq. (1). With the measured relative intensity of several emission lines,

and the use of NIST data base, a Boltzmann plot of the $ln\left(\frac{\lambda I}{A_{ki}g_k}\right)$ term of emission lines against E_k can be obtained. The slope of a straight line is equal to $(1/kT_e)$. Te can thus easily be obtained from the slope inverse.

4.3. Electron Density Calculations

Figure 6 depicts the peak profile of the 538.63 nm Fe I line. The full width at half maximum was determined via Lorentz fitting. For the various meteorite samples, the observed width is dependent on the Stark effect and the standard line width, which is 0.0212 nm. An increase in electron density may be seen in the widening of the entire breadth.

5. Results and Discussion

First, using good-resolution spectroscopy and a CCD camera with the same design and technical specifications as those used for meteor observation, one can record the spectrum of the evaporation plasma of four meteorite samples: Draconids, Hydrids, Virginids, and sporadic meteors. The emission spectra of the plasma produced at the Fe I generated by these meteoroids were recorded. Figure 1 shows the recorded spectra of different meteorites. Using the (EDMOND) database, a spectrum can be chosen for the meteorites under study. One can allocate and assemble 34 spectral lines with suitable intensity for these meteorites. Thorlabs software is used to calculate Lorentz fittings, and use the NIST Atomic Spectra Database for getting emission lines parameters. 13 of the lines in this list can be deemed notable. Figure 1 highlights the locations of the most significant spectrum lines. Strong series of Fe I and Cr I lines, many strong lines of Al I, Mg I, Si I, and Na I, and lesser emissions of Mn I, Ti I, and Ni I make up the major spectral lines of neutral elements. Additionally, ions of Ca II and Mg II have been observed by [25], [26]. In fact, our qualitative examination of the ablation spectra agrees exactly with that which was reported by [27]. The presence of Fe I lines in the short wavelength region is possible. Four Fe I lines with wavelengths of (438.85, 499.97, 538.7, and 544.1) nm were investigated for measuring electron temperature and density as a function type of meteorite. The parameters of these lines can be obtained from NIST database, as noted in Table 1.

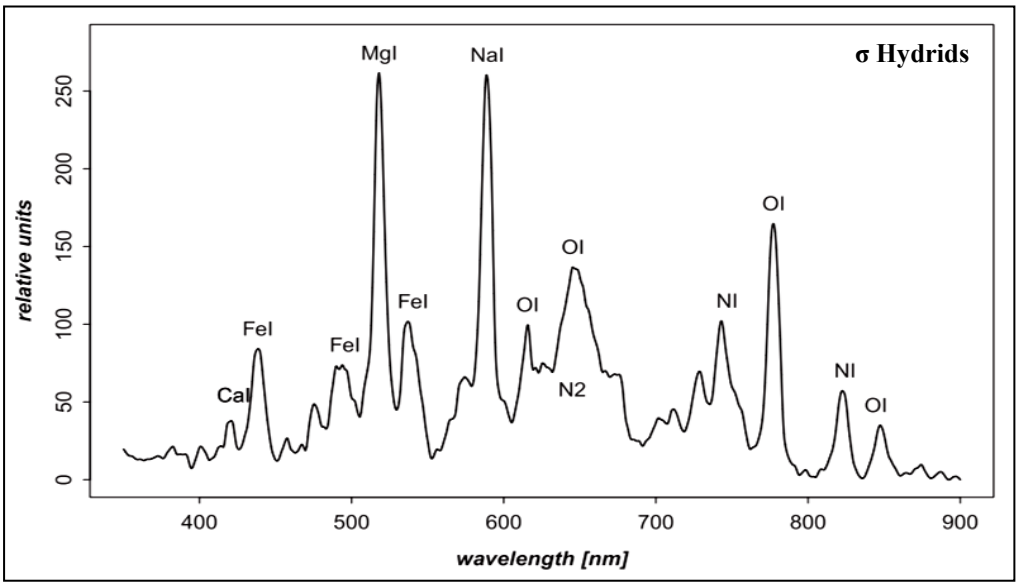

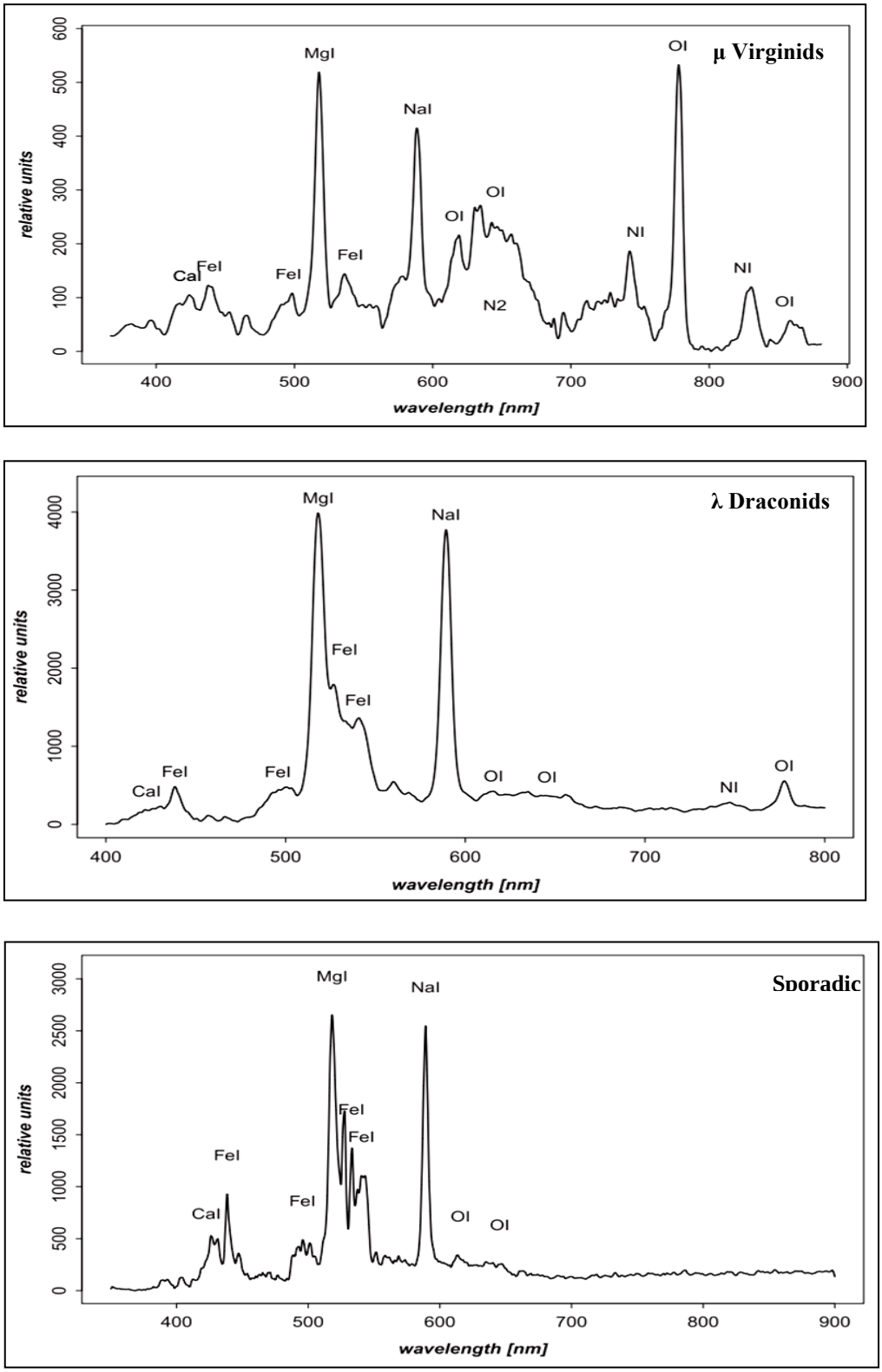

Figure 1: Samples of meteor spectra of λ Draconids, σ Hydrids, μ Virginids, and sporadic meteor (Nos. 1, 3, 8, and 32, respectively) [13].

The appearance of dots on a straight line with a slope signifying the electron temperature is obvious since C in the LTE model that is so tiny, therefore it's neglected. The electron temperature is determined for several meteorites, as seen in Figure 2. The slope in the Boltzmann plot agrees with the temperatures 0.147 eV for λ Draconids, 0.148 eV for σ Hydrids, 1.432 eV for μ Virginids, and 1.241 eV for Sporadic meteors. The results of our spectra structure are listed in Table 1. This method's direct estimation of electron temperature agrees well with previous research [28].

Table 1: Results of our spectra analysis

Wavelength [λ Draconids]	**A g**	**E_j**	**E_k**	**Intensity Fe I**
438,85	$7.21x10^7$	3.60252504	6.42699840	85,18
499,97	$5.1x10^6$	4.18636440	6.66579718	74.74
538,7	$2.12\ x10^6$	4.14264893	6.44334733	100
544.1	$4.5\ x10^6$	4.31247059	6.59039805	50
Wavelength [σ Hydrids]	**A g**	**E_j**	**E_k**	**Intensity Fe I**
437.5	$1.38\ x10^6$	3.57321890	6.40603863	122.72
497.5	$3.3\ x10^7$	3.95972364	6.45212430	109.09
537.5	$1.2\ x10^6$	4.29441489	6.59967157	140.90
555	$8.9\ x10^6$	4.43461275	6.66650376	86.355
Wavelength [μ Virginids]	**A g**	**E_j**	**E_k**	**Intensity Fe I**
438.78	$1.04\ x10^7$	3.07133880	5.89614419	499.99
502,04	$1.68\ x10^6$	2.99035244	5.45809748	464.28
526.72	$9.90\ x10^7$	3.26570610	5.35157038	1785,71
540.8	$9.30\ x10^6$	4.38646275	6.67955657	1357.14
Wavelength [sporadic meteor]	**A g**	**E_j**	**E_k**	**Intensity Fe I**
438.4	$2.7\ x10^6$	3.01725044	5.84412959	925
497.28	$4.91\ x10^6$	3.63521992	6.12892712	475
525.3	$6.45\ x10^6$	3.28302483	5.64241573	1725
533.28	$2.0\ x10^6$	4.18636440	6.51071489	1375

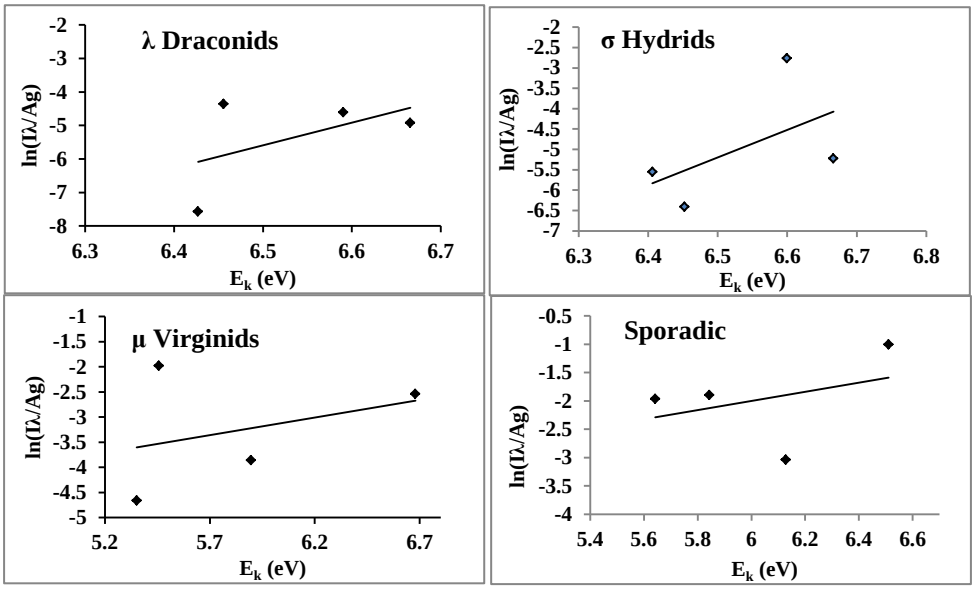

Figure 2: The Boltzmann plot for Fe I lines at different meteorites.

For all of the ablation spectra, Figure 3 depicts the fit of Lorentzian of the Fe I emission lines at 538.63 nm. These values and the $\lambda_{1/2}$ of this line is utilized in all four observations meteorites, and calculated using the fit and the line parameter which was determined to be w = 0.0212 nm for this clearly discernible line nm [21].
We got from Eq. (2) a mean electron density of all meteorites, which is reported in Table 2. On the basis of these results, we can state that the McWhirter criterion for the LTE plasma is verified. Particular results for each meteorite are shown in Figure 3.

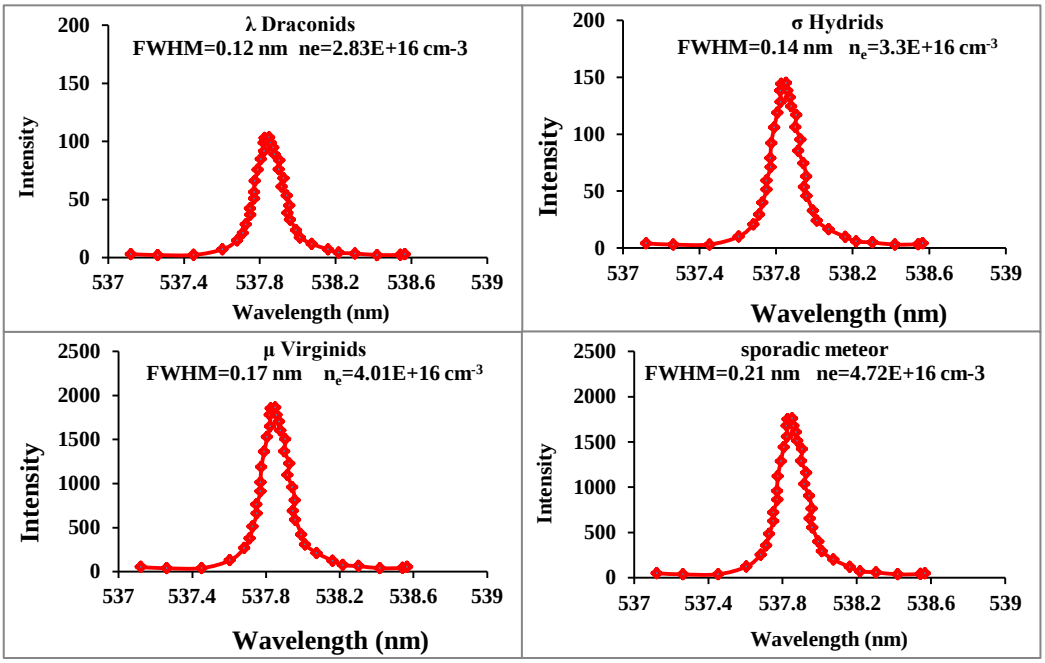

Figure 3: The Lorentzian fit of the Fe I 538.63 nm emission lines for all the ablation spectra.

Table 2: Plasma parameters of four meteorites

Meteorites	Electron Temperature T_e eV	Electron Density n_e cm^{-3}	Debye length cm	Plasma frequency rad/sec
λ Draconids	0.147	$2.83x10^{16}$	$1.69338x10^{-05}$	$2.08x10^{10}$
σ Hydrids	0.148	$3.3x10^{16}$	$1.57349x10^{-05}$	$2.24x10^{10}$
μ Virginids]	1.432	$4.01x10^{16}$	$4.44005x10^{-05}$	$2.47x10^{10}$
sporadic meteor	1.241	$4.72x10^{16}$	$3.80981x10^{-05}$	$2.68x10^{10}$

6. Conclusions

First findings from the newly started meteor spectroscopic study presented in this article show how the addition of spectroscopic cameras considerably increases the amount of meteor data that can be gathered. Spectroscopy analysis is a useful technique for comprehending meteoroids and their parent bodies. In this study, a sample of meteor spectra that had been captured by the AMOSSpec camera, since November 2013, was analyzed. The following are the key conclusions of this study:

All spectra are drawn in one Boltzmann plot, and the temperatures of electrons were determined using the high shining Fe I spectral lines and were as follows: 0.147, 0.148, 1.432, and 1.241 eV for λ Draconids, σ Hydrids, μ Virginids, and Sporadic meteors, respectively. The data are compared with those of other authors. All results are in good agreement with the previous work.

References

[1] V. Dmitriev, V. Lupovka and M. Gritsevich, "Orbit determination based on meteor observations using numerical integration of equations of motion," Planetary and Space Science, vol. 117, p. 223–235, 2015.

[2] J. M. and C. Plane, "Cosmic dust in the earth's atmosphere," Chem. Soc. Rev., vol. 41, p. 6507–6518 , 2012.

[3] O. Kalashnikova, M. Horgnyi, G. E. Thomas and a. O. B. Toon., "Meteoric smoke production in the atmosphere," Geophysical Research Letters, vol. 27, no. 20, pp. 3293-3296, 2000.

[4] E. A. Silber, M. Boslough, W. K. Hocking, M. Gritsevich and R. W. Whitaker., "Physics of meteor generated shock waves in the Earth's atmosphere – A review," Advances in Space Research, vol. 62, no. 3, pp. 489-532, 2018.

[5] L. A. R. K. A. Hill And R. L. Hawkes., "Sputtering And High Altitude Meteors," Earth, Moon, And Planets , Vol. 95, PP. 403-412, 2004.

[6] I. Safii., "Recent aspects concerning DC reactive magnetron sputtering of thin films: a review.," Surface and Coatings Technology ., vol. 127., pp. 203-219., 2000. .

[7] T. Vondrak1, J. M. C. Plane1, S. Broadley1 and a. D. Janches2., "A chemical model of meteoric ablation.," Atmos. Chem. Phys., vol. 8., p. 7015–7031., 2008..

[8] I. Williams., "The Evolution of Meteoroid Streams.," ASP Conference Series., vol. 104., pp. 88-99, 1996..

[9] Z. C. a. J. Í. Borovicˇka, W. G. Elford, D. O. Revelle, R. L. Hawkes, V. Porubcan And M. Šimek., "Meteor Phenomena And Bodies," Space Science Reviews , vol. 84. , p. 327–471., 1998..

[10] L. Rogers, K. A. Hill and a. R. Hawkes, Mass Loss Due to Sputtering and Thermal Processes in Meteoroid Ablation, vol. 41., Sackville, NB Canada: Planetary and Space Science, 2004, p. 6507–6518..

[11] O. P. Popova, S. N. Sidneva, A. S. Strelkov and V. V. Shuvalov, "Formation of disturbed area around fast meteor body," European space Agency., vol. 38, pp. 495-237, 2001.

[12] S. Abe, N. Ebizuka, K. O. Hideyuki Murayama, S. Sugimoto, M.-Y. Yamamoto, H. Yano, J.-I.

Watanabe And J. I. B. Ka., "Video And Photographic Spectroscopy Of 1998 And 2001 Leonid Persistent Trains From 300 To 930 Nm.," Earth, Moon, And Planets, Vol. 95., P. 265–277., 2004..

[13] J. B. a. H. Betlem., "Spectral analysis of two Perseid meteors," Planet. Space Sci., vol. 45. , no. 5, pp. 563-575., 1997..

[14] M. Ferus, J. Koukal, L. Lenža, J. S. P. Kubelík, V. Laitl, E. M. Zanozina, P. Váňa, T. Kaiserová, A. Knížek and a. S. Civiš, "Recording and Evaluation of High Resolution Optical Meteor Spectra and Comparative Laboratory Measurements Using Laser Ablation of Solid Meteorite Specimens," in Conference: 2017 19th International Conference on Transparent Optical Networks (ICTON), Girona, Spain, 2017.

[15] P. M. Millman, "A general survey of meteor spectra," Smithsonian Contributions to Astrophysics, vol. 7, pp. 119-127, 1963.

[16] J. Zender, D. Koschny, O. Witasse and M. D. Campbell-Brown, "Video intensified camera setup of visual and meteor spectroscopy.," EARTH PLANETS SPACE., 2004..

[17] W. I. Yaseen, A. F. Ahmed, D. A. Al-Shakarchi and F. A. Mutlak., "Development of a high-power LC circuit for generating arc plasma and diagnostic via optical emission spectroscopy.," Applied Physics A, vol. 25, pp. 128-148, 2022..

[18] I. P. Herman., "Optical Diagnostics for Thin Film Processing.," Academic Press., vol. 7, pp. 24-28, 1996..

[19] A. D. Giacomo., "A novel approach to elemental analysis by Laser Induced Breakdown Spectroscopy based on direct correlation between the electron impact excitation cross section and the optical emission intensity.," Spectrochimica Acta Part B, vol. 66., p. 661–670., 2011..

[20] F. J. Moaen and H. R. Humud., "Spectroscopic and Thermal Properties for Exploding Silver Wire Plasma in Deionized Water.," Iraqi Journal of Science., vol. 63., no. 12., pp. 5208-5217., 2022..

[21] A. L. N. Konjevi, J. R. Fuhr and a. W. L. Wiese., "Experimental Stark Widths and Shifts for Spectral Lines of Neutral and Ionized Atoms (A Critical Review of Selected Data for the Period 1989 Through 2000).," Journal of Physical and Chemical., vol. 31., no. 3., pp. 819-927., 2002..

[22] A. A.-K. Hussain, K. A. Aadim and W. I. Yaseen., "Diagnostics of low-pressure capacitively coupled RF discharge argon plasma.," Iraqi Journal of Physics., vol. 13., no. 27., pp. 76-82., 2015..

[23] K. A. Aadim., "Characterization of Laser induced cadmium plasma in air.," Iraqi Journal of Science., vol. 56., no. 3., pp. 2292-2296., 2015..

[24] H. R. H. a. S. Hussein., "Optical emission spectroscopy for studying the exploding copper wire plasma parameters in distilled water.," Iraqi Journal of Physics., vol. 15., no. 35., pp. 142-147., 2017..

[25] "Mineralogy, petrography, geochemistry, and classification of the Kosice meteorite.," Meteoritics & Planetary Science, vol. 50., no. 5., p. 864–879., 2015..

[26] Dell'Aglio, M. Giacomo, A. De, R. Gaudiuso, O. D. Pascale, G. Senesi and a. S. Longo, "Laser Induced Breakdown Spectroscopy applications to meteorites: Chemical analysis and composition profiles.," Geochimica et Cosmochimica., vol. 74., p. 7329–7339., 2010..

[27] J. Borovi˘cka., "Physical and chemical properties of meteoroids as deduced from observations.," International Astronomical Union., vol. 229., pp. 251-271., 2006..

[28] J. M. Trigo-Rodr´ıguez, J. Llorca2 and a. J. Fabregat., "Chemical abundances determined from meteor spectra – II. Evidence for enlarged sodium abundances in meteoroids.," Mon. Not. R. Astron. Soc., vol. 348., p. 802–810., 2004..